Title

Investigation of HVAC operation strategies for office buildings during COVID-19 pandemic

Authors

Faulkner, Cary A

Castellini, John E

Zuo, Wangda

et al.

Publication Date

2022

DOI

10.1016/j.buildenv.2021.108519

Since January 2020 Elsevier has created a COVID-19 resource centre with free information in English and Mandarin on the novel coronavirus COVID-19. The COVID-19 resource centre is hosted on Elsevier Connect, the company's public news and information website.

Building and Environment 207 (2022) 108519

Contents lists available at ScienceDirect

Building and Environment

journal homepage: www.elsevier.com/locate/buildenv

Investigation of HVAC operation strategies for office buildings during COVID-19 pandemic

Cary A. Faulkner [a], John E. Castellini Jr. [a], Wangda Zuo [a,b,c,*], David M. Lorenzetti [d], Michael D. Sohn [d]

[a] Department of Mechanical Engineering, University of Colorado Boulder, UCB 427, Boulder, 80309, CO, USA
[b] Department of Civil, Environmental and Architectural Engineering, University of Colorado Boulder, UCB 428, Boulder, 80309, CO, USA
[c] National Renewable Energy National Laboratory, Golden, 80401, CO, USA
[d] Energy Analysis and Environmental Impacts Division, Lawrence Berkeley National Laboratory, 1 Cyclotron Road, Berkeley, 94720, CA, USA

ARTICLE INFO

Keywords:
COVID-19
Indoor air quality
Building energy
Modelica

ABSTRACT

To minimize the indoor transmission of contaminants, such as the virus that can lead to COVID-19, buildings must provide the best indoor air quality possible. Improving indoor air quality can be achieved through the building's HVAC system to decrease any concentration of indoor contaminants by dilution and/or by source removal. However, doing so has practical downsides on the HVAC operation that are not always quantified in the literature. This paper develops a temporal simulation capability that is used to investigate the indoor virus concentration and operational cost of an HVAC system for two mitigation strategies: (1) supplying 100% outdoor air into the building and (2) using different HVAC filters, including MERV 10, MERV 13, and HEPA filters. These strategies are applied to a hypothetical medium office building consisting of five occupied zones and located in a cold and dry climate. We modeled the building using the Modelica *Buildings* library and developed new models for HVAC filtration and virus transmission to evaluate COVID-19 scenarios. We show that the ASHRAE-recommended MERV 13 filtration reduces the average virus concentration by about 10% when compared to MERV 10 filtration, with an increase in site energy consumption of about 3%. In contrast, the use of 100% outdoor air reduces the average indoor concentration by about an additional 1% compared to MERV 13 filtration, but significantly increases heating energy consumption. Use of HEPA filtration increases the average indoor concentration and energy consumption compared to MERV 13 filtration due to the high resistance of the HEPA filter.

1. Introduction

The COVID-19 pandemic has increased the need for buildings to improve their indoor air quality to help reduce the risk of infection from airborne transmission. A recent study [1] found that all 318 identified outbreaks of three or more COVID-19 cases in China occurred in indoor environments. Another study [2] found an outbreak of 55 cases among 81 attendees of in-person exercise classes at an indoor facility in Chicago, IL. It was also found that the direction of the airflow due to the air-conditioning system played a large role in the infection of patrons inside a restaurant in Guangzhou, China [3]. These studies demonstrate the significant risk of indoor infection. As a result, organizations, such as ASHRAE in January 2021 [4], provided recommendations for building operation during the pandemic to improve indoor safety. Included were recommendations for the heating, ventilation, and air conditioning (HVAC) system operation, such as providing necessary ventilation and using filters that achieve minimum efficiency reporting value (MERV) 13 or better. The recommended strategies have been shown to be helpful in improving indoor air quality, but their impacts on the HVAC system operation, such as energy consumption, are not quantified and need to be investigated further.

Previous literature tried to study and compare strategies to improve indoor air quality to better understand this issue. Zhang et al. [5] conducted experimental studies to investigate the effectiveness of different HVAC filters to remove airborne viral particles. They found the viral filtration efficiency generally correlated with the filter MERV rating and high-efficiency filters were effective at capturing airborne viral particles. Zaatari et al. [6] studied the effect of filter pressure drop on energy consumption and clean-air-delivery-rate. They found replacing a MERV 8 filter with MERV 13/14 filter for a system in

* Correspondence to: ECCE 247, UCB 428, 1111 Engineering Dr., Boulder, CO 80309, USA.
E-mail address: wangda.zuo@colorado.edu (W. Zuo).

https://doi.org/10.1016/j.buildenv.2021.108519
Received 28 July 2021; Received in revised form 11 October 2021; Accepted 26 October 2021
Available online 12 November 2021

fan-only mode with fan speed control increased energy consumption by 11%–18% but improved clean-air-delivery-rate by a factor of 2.9–3.8. Santos and Leal [7] characterized the relationship between energy consumption and ventilation rates in European buildings and found increasing ventilation rates can significantly impact annual building energy use. Other studies [8,9] compared the impact of different levels of ventilation and filtration on indoor $PM_{2.5}$ concentration and financial cost. Azimi and Stephens [10] studied risk reduction of influenza virus and associated operational costs for different filter ratings and equivalent levels of outdoor air ventilation. In addition, they found filtration improved risk reduction with lower costs compared to increased ventilation. A study during the COVID-19 pandemic [11] found that, when sleeping in the same room as an infected person, running the fan of the air-conditioning system can lower the risk of infection by one-third and improving system filtration can reduce the risk by two-thirds. Pease et al. [12] investigated the effect of filtration, air change rate, and outdoor air fraction on the concentration of COVID-19 virus and probabilities of infection in a multi-room building. They found filtration was the best method for reducing virus concentration. The study also suggested that although increasing outdoor air rate or air change rate is proved to be beneficial, they should be used with caution. For example, increasing the outdoor air rate can increase the heating or cooling energy used by the HVAC system due to the temperature difference between the indoor and outdoor air.

Although significant progress has been made in the literature, further improvements can be made. First, current studies lack detailed modeling of the operation and control of the HVAC system, for example by assuming constant ventilation rates. As a result, the dynamic effects of the HVAC system, which are critical for real system operation, are lost. For example, the controls of the outdoor air damper and supply fan can affect the dilution and removal rate of indoor virus concentration as well as the HVAC energy consumption. Also, many studies evaluate risk with steady-state concentrations and constant occupancy, while both these values are dynamic in practice. Additionally, the supply fan in the HVAC system is often assumed to be sized to accommodate the additional pressure drop of high-efficiency filters. However, in reality a building's HVAC system may not be sized to replace their existing HVAC filter with a more efficient filter that increases the system pressure drop. Finally, while some of these studies perform annual simulations, they do not compare the indoor air quality and their associated operational cost during different times of the year. The effect of outdoor conditions can determine the optimal operating strategy, which may vary over the course of the year.

To address this gap, we use an equation-based, object-oriented modeling language (Modelica) to develop a detailed model of an HVAC system and enable temporal analyses. For example, Fu et al. [13] used Modelica-based models to study cooling systems in data centers and investigate their performance during normal and emergency conditions. Huang et al. [14] used Modelica-based models to study control related faults for chiller and boiler plants. Tian et al. [15] used computational fluid dynamics coupled with Modelica to optimize thermostat placement in an office room based on thermal comfort and energy consumption. The efficient dynamic modeling offered by Modelica language, as well as the availability of the Modelica *Buildings* library [16,17], were enabling features to these studies. Additionally, our developed models for HVAC filters and virus transmission, to our knowledge, have not yet been created using a Modelica-based platform.

The remainder of this paper is organized as follows. First, a review of HVAC operation strategies to reduce the risk of transmission of airborne virus indoors is presented in Section 2. Next, the implementation of new models for HVAC filters and virus transmission into an existing Variable Air Volume (VAV) system model for a medium office building is detailed in Section 3. Then, results for virus concentration and energy consumption for the different strategies are shown and the combined results are analyzed in Section 4. Finally, the paper is concluded in Section 5.

2. Review of HVAC operation strategies to mitigate indoor disease transmission

There are several methods to improve indoor air quality by HVAC operation, each with different benefits and drawbacks. Guo et al. [18] summarized and compared HVAC operation guidelines during the COVID-19 pandemic for buildings in different countries. Based on this review, common strategies include: (1) increasing ventilation rates of outdoor air as high as possible, (2) running the HVAC system for longer periods to flush out lingering virus, and (3) improving filtration of recirculating air. Increasing the supply rate of outdoor air can dilute the indoor concentration of virus without the need of purchasing and maintaining new equipment, as well as without increasing the system pressure drop in the air handling system. However, increasing the supply flow rate of outdoor air can significantly increase cooling or heating energy consumption when the outdoor air temperature differs greatly from the room temperature setpoint. It may also sacrifice the thermal comfort as most HVAC systems are not sized for higher outdoor airflow rates than the design. Secondly, increasing the runtime of the HVAC system, for example running the system longer before or after occupants arrive, can help flush out virus lingering in the room. Finally, improving the filtration of recirculating air can reduce virus concentration without increasing heating or cooling energy consumption due to increased ventilation. However, the airflow resistance caused by HVAC filters may increase the pressure drop through the air handling system, which could increase fan energy consumption and/or reduce the system flow rate [6]. Furthermore, there are associated financial costs of purchasing and installing the HVAC filters, as well as replacing the filter after it accumulates particles over time.

This review suggests that mitigation strategies might benefit, or differ, if an evaluation considered the typical change in occupancy, as well as cooling and heating loads, over the course of a day. Thus, this paper studies the strategies of supplying 100% outdoor air and using high-efficiency HVAC filters, since these strategies can be used to improve the indoor air quality throughout the day. There are many HVAC filters that are often defined using MERV, which describes their ability to filter particles of different sizes [19]. ASHRAE recommends [4] to use filtration that achieves at least MERV 13 during the pandemic due to their ability to filter at least 85% of airborne particles with diameter between 1–3 μm. The most efficient filters are known as high-efficiency particulate absorbing (HEPA) filters, which exceed MERV 16 and filter 99.97% of airborne particles with diameter at 0.3 μm [20]. Thus, this paper investigates the use of MERV 13 and HEPA rated filters, representing the minimum recommended rating for use during the pandemic and the maximum achievable rating. These strategies are evaluated against MERV 10 filtration, which filters at least 50% of airborne particles with diameter between 1–3 μm [19] and may be used in older buildings. It should be noted the 100% outdoor air strategy is assumed to use a MERV 10 filter, since buildings use HVAC filters to filter outdoor air as well.

3. Model implementation

For the temporal simulations, we first developed a temporal simulation of a variable-air-volume (VAV) HVAC supply system for a typical medium office building. We based the building model along a prototype provided in the Modelica *Buildings* library [21]. For our simulations, we developed modules to supplement the prototype to represent HVAC filtration and virus transmission. In this section, we describe the features of the model of the medium office building and our qualitative verification of the new models to support this study. Finally, we describe the whole building model with the new modules incorporated.

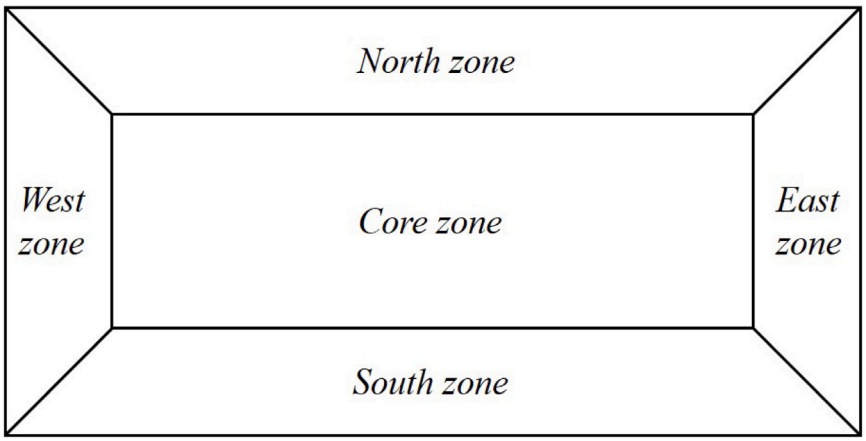

Fig. 1. Floor layout of the medium office building with five zones.

3.1. Overview of the building system

This building was based on the DOE commercial reference medium office building [22], with focus on the bottom floor building prototype. The floor contains five zones, including a core zone and four perimeter zones, as shown in Fig. 1. These zones are assumed to be well-mixed in the model, with volumes of 2698 m^3 for the Core Zone, 569 m^3 for the North and South zones, and 360 m^3 for the East and West zones. We have a central air handling unit with heating and cooling coils with VAV terminal boxes containing reheat coils in each zone. An outdoor air economizer is used to provide fresh, outdoor air to the building and is controlled to supply at least the minimum outdoor airflow based on the ASHRAE standard [23]. Additional outdoor air may be supplied to provide free cooling. The HVAC system is sized for the location of Denver, Colorado. Cooling is provided using chilled water with coefficient of performance of 5, which is defined as the ratio of the rate of cooling provided to the input electrical power. Heating is provided using a hot water system with efficiency of 0.8, which is the ratio of the rate of heating provided to the input required power. The system is controlled based on the control sequence VAV 2A2-21232 from the Sequences of Operation for Common HVAC Systems described in [24].

3.2. Implementation of new models

The development of the new models to support this study are detailed next. First, the new HVAC filter component model is described, followed by the models for virus generation and decay. The new models are also qualitatively verified.

3.2.1. HVAC filter model

An HVAC filter model was developed to support the work for this paper, since such a model was not included in the original VAV system model. The model includes two main components: removal of virus based on a defined efficiency and static pressure drop depending on the mass flow rate and defined nominal flow conditions.

The removal of virus can be described as:

$$c_{out} = (1 - \eta_{filter})c_{in}, \tag{1}$$

where c_{out} is the virus concentration exiting the filter, η_{filter} is the filter removal efficiency in terms of percentage of virus removed, and c_{in} is the virus concentration entering the filter. The filter efficiency can be between 0%–100%, where $\eta_{filter} = 100\%$ describes a filter that completely removes all virus in the airflow.

The removal of virus for the HVAC filter model was qualitatively verified with a simple unit study, by supplying air with concentration c_0 to a room initially virus free for different filter efficiencies. The case was run for 500 s, when the concentrations approach their equilibrium values. The results in Fig. 2 show the normalized concentrations approach their expected steady-state values of $(1-\eta_{filter})c_0$, since the filter removes a fraction of η_{filter} from the supply flow with concentration c_0. This confirms the HVAC filter model removes virus as expected based on Eq. (1).

Next, the static pressure drop caused by the resistance of the filter is:

$$\Delta p_{filter} = k_{filter}\dot{m}^2_{filter}, \tag{2}$$

where Δp_{filter} is the static pressure drop caused by the filter, $\dot{m}_{filter}$ is the mass flow rate of air though the filter, and k_{filter} is:

$$k_{filter} = \frac{\Delta p_{nom}}{\dot{m}^2_{nom}}, \tag{3}$$

where Δp_{nom} is the nominal pressure drop at the nominal mass flow rate, $\dot{m}_{nom}$. These two values are inputs to the filter model. The quadratic relation between static pressure drop and mass flow rate can be approximated using the Bernoulli equation and captures the general trend from experimental data [19]. It should be noted that the filter pressure drop increases over time as the filter collects particles [25], but the nominal pressure drop was assumed to be constant in this study for simplicity.

The pressure drop as a function of flow rate for the HVAC filter model was demonstrated by supplying air at rates of 0.5 kg/s - 1.5 kg/s with different filter nominal pressure drops. The nominal mass flow rate for the filter was held constant at 1.0 kg/s for all the cases. The results output from the model are shown in Fig. 3.

The results confirm the expected quadratic relation between pressure drop and mass flow rate based on Eq. (2). It can also be seen that the pressure drops for the three cases pass through their nominal values at the nominal mass flow rate of 1.0 kg/s.

The settings used for the filters used in this study are shown in Table 1. The filter efficiencies come from ASHRAE technical resources [19] and the nominal pressure drop values are chosen based on data for MERV 10 [26], MERV 13 [27], and HEPA [10] filters based on the nominal flow rate of the studied system. The pressure drop can vary for filters with the same rating based on the filter type and depth of the filter [9]. The pressure drop also increases over time

Table 1
HVAC filter simulation settings.

Filter	Nominal Pressure Drop (Pa)	Efficiency
MERV 10	143	50%
MERV 13	162	85%
HEPA	373	99.97%

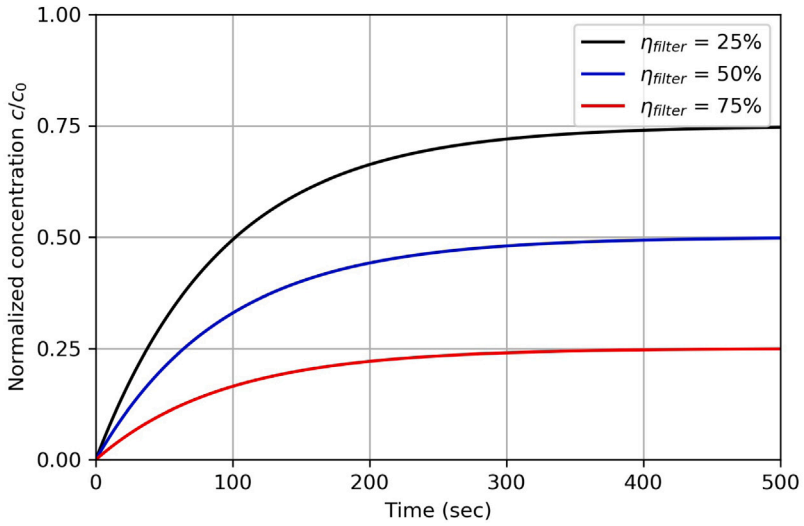

Fig. 2. Normalized room virus concentrations over time with different HVAC filter efficiencies.

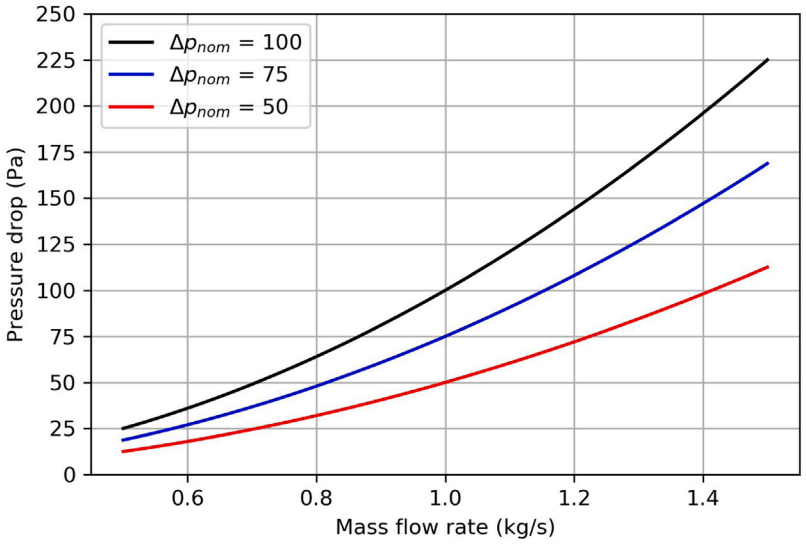

Fig. 3. Filter pressure drop vs mass flow rate for different nominal pressure drops.

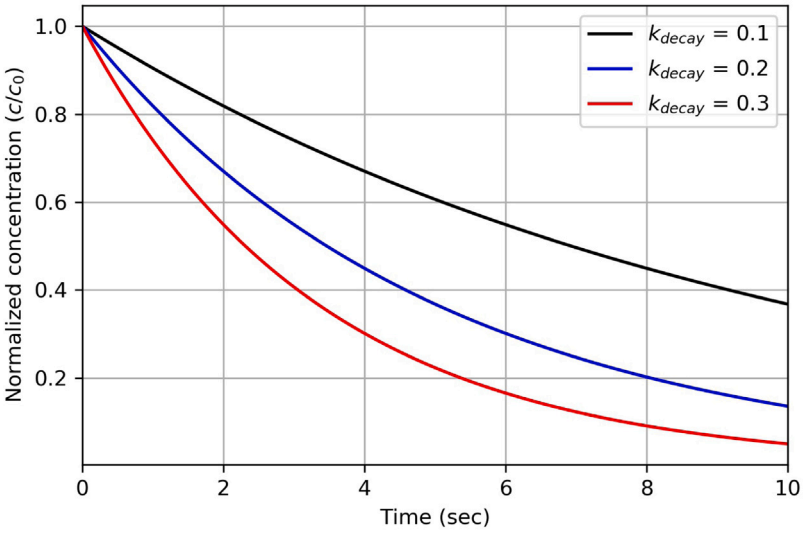

Fig. 4. Normalized virus concentration over time with different viral decay rate values.

as the filter accumulates particles. Thus, the nominal pressure drops shown in Table 1 are chosen based on the average between the typical initial pressure drop of the clean filter and the final pressure drop recommended by the manufacturer.

3.2.2. COVID-19 virus modeling

Additionally, models for the generation and decay of virus in the rooms were developed for this study. First, we simulated the presence of one "sick" person in each zone working from 9:00 AM to 5:00 PM, Monday through Friday throughout the year. The purpose of the presence of sick people throughout the year was to study the concentrations and effect of strategies in all the zones during the different seasons. Generation of virus was described in terms of quanta emission rates, where a quantum is the dose of airborne droplet nuclei expected to cause infection in 63% of susceptible people. Quanta emission rate of COVID-19 virus is difficult to quantify and dependent on many uncertain values, such as viral load in the mouth and activity level of the sick person [28]. We use a value of 25 quanta/h for the majority of the study based on literature [28,29], although different quanta emission values are considered in Section 4.1.3 to compare the risk of infection for different emission rates. The virus was generated directly in each well-mixed zone when the sick people were present based on the quanta emission rate.

The viral decay in the room due to gravitational settling and the death of airborne viruses is modeled based on Eq. (4), which has been used in literature to model viral decay in well-mixed zones [12]. This is described as:

$$\dot{c}_{decay,zone} = k_{decay} c_{zone}, \tag{4}$$

where $\dot{c}_{decay,zone}$ is the rate of viral decay in the zone, k_{decay} is a defined constant rate of viral decay, and c_{zone} is the virus concentration in the zone.

The decay model was qualitatively tested by examining the viral decay in a room with initial concentration c_0. There were no other means to produce or remove virus, other than loss due to a holistic decay rate. For this case, the virus concentration in the room can be derived analytically as:

$$c(t) = c_0 \exp(-k_{decay} t), \tag{5}$$

where $c(t)$ is the transient virus concentration in the room, c_0 is the initial virus concentration, k_{decay} is the viral decay rate, and t is time. The results for virus concentration over time with different viral decay rates are shown in Fig. 4. The results match the expected trend of the virus concentration decaying exponentially and faster for larger values of k_{decay}.

To quantify the impact of the virus concentrations, risk of infection is calculated using the Wells–Riley approach, which determines this risk based on the amount of virus inhaled by an occupant. Risk of infection is calculated as:

$$R(t) = 1 - \exp(-IR \int_{t_0}^{t} c(t)\, dt), \tag{6}$$

where $R(t)$ is risk of infection in terms of percentage, IR is the volumetric inhalation rate of air for an occupant, and $\int_{t_0}^{t} c(t)\, dt$ is the integral of virus concentration in the room with respect to time since initial time t_0. The predicted number of infections, R_0, can be calculated based on the risk, R. The predicted number of infections over time, $R_0(t)$ is calculated accounting for the variable occupancy in the zone for this study. This is done by calculating $R_0(t)$ for a given time interval when the occupancy is constant and adding the predicted number of infections calculated from the previous time interval. This can be described as:

$$R_{0,T}(t) = S_T[1 - \exp(-IR \int_{t_0}^{t} c(t)\, dt)] + R_{0,T-1}(t_0), \tag{7}$$

where $R_{0,T}(t)$ is the predicted number of infections in the zone for time interval T, S_T is the number of susceptible occupants in the zone during T, t_0 is the time at the beginning of interval T, and $R_{0,T-1}(t_0)$ is the predicted number of infections from the previous time interval, $T-1$, ending at time t_0. Susceptible occupants is determined as $S = N - 1$, where N is the number of occupants. This way S does not account for the sick person, since they cannot infect themselves. Fig. 5 shows the predicted number of infections for a sample day based on the virus concentration and occupancy. A sample time interval, T, is highlighted to show how R_0 is calculated based on the number of susceptible occupants and amount of inhaled virus during this time. At the beginning of this time interval, the slope of $R_0(t)$ initially increases

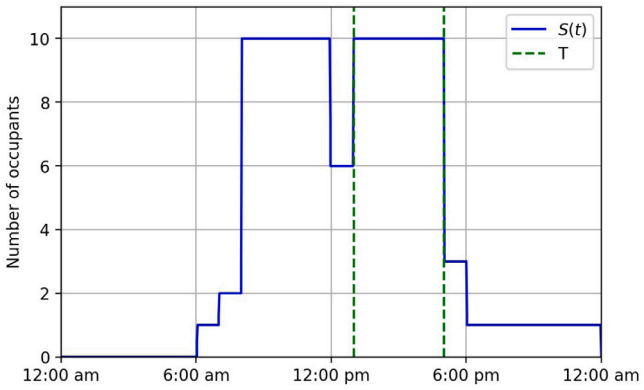

(a) Occupancy during the day.

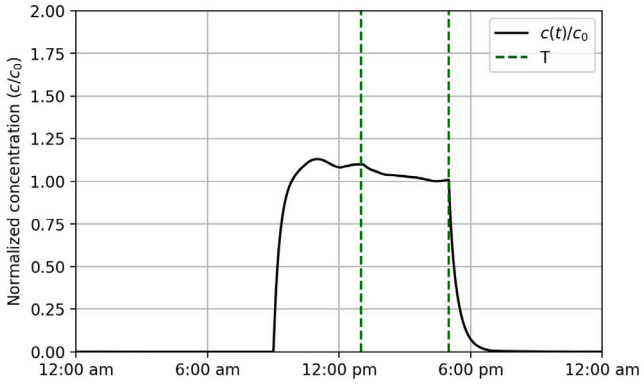

(b) Normalized virus concentration.

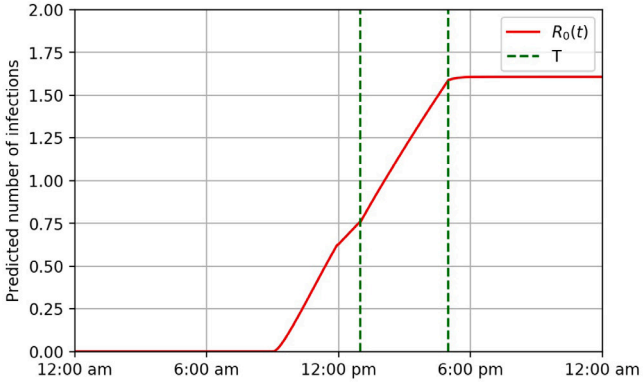

(c) Predicted number of infections.

Fig. 5. Predicted number of infections based on the occupancy and virus concentration for a sample day.

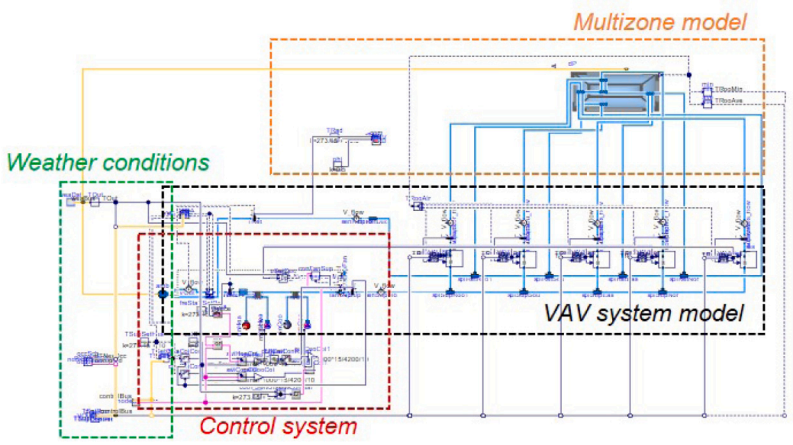

Fig. 6. Modelica model of the medium office building.

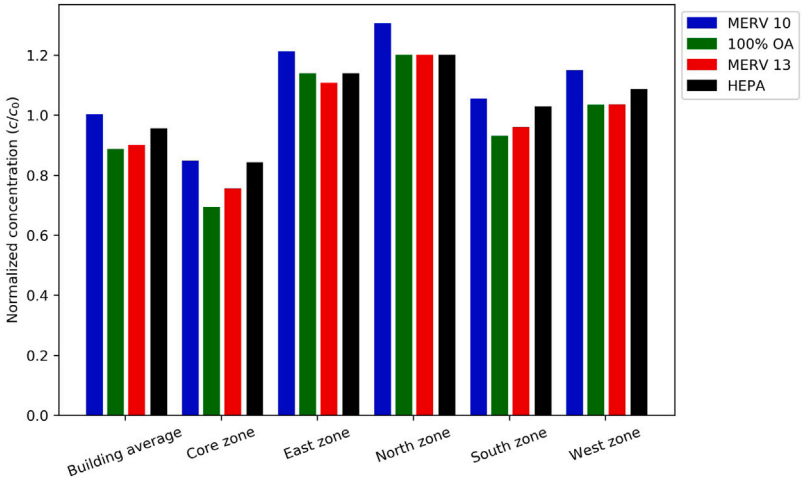

Fig. 7. Annual-average, normalized virus concentration results for the different strategies and zones.

due to the increase in occupancy as the susceptible occupants return from lunch. $R_0(t)$ then steadily increases as occupants constantly inhale virus in the zone. Finally, $R_0(t)$ quickly flattens out after this interval as occupants leave and the virus concentration decreases. For this study, the values for viral decay and inhalation rate were chosen to be 0.48 h^{-1} and 0.48 m^3/h based on literature [12].

3.3. Whole building model

The newly developed models were added to the VAV system model to perform this study and the final Modelica model capability is shown in Fig. 6. The entire model can be divided into four sections: (1) the multizone airflow model for the five zones, which includes the generation and decay of virus in the zones; (2) the VAV system model which includes the central air handling unit, as well as VAV terminal boxes and the return duct; (3) the control system which includes PI controllers for the heating and cooling coils, outdoor air economizer, and supply fan; and (4) the weather conditions, including dry bulb temperature, wind speed, and radiative exchange.

4. Results and discussions

In this section, the results for indoor virus concentration are presented first, followed by the results for energy consumption. Finally, analysis of the combined results is performed to consider best overall strategies based on both indoor air quality and operational cost.

4.1. Virus concentration results

The virus concentration results are presented for different time scales in this section. First, the annual average virus concentration results in the five zones for the different strategies are presented. Next, the monthly average results are presented to show how the concentrations vary throughout the year. It is worth noting that the annual and monthly averages only account for the concentrations during occupied hours. Finally, results from two sample days are presented including risk analysis based on predicted number of infections.

4.1.1. Annual virus concentration results

The results of the annual-average virus concentration by four different strategies in five different zones are shown in Fig. 7. The indoor virus concentration results in this figure and throughout this section are normalized by c_0, which is the building average virus concentration for the MERV 10 case (first blue bar on the left in Fig. 7). The results show that the strategy of supplying 100% outdoor air provides the lowest annual building-average virus concentration and reduces the annual building-average virus concentration by about 11% compared to using MERV 10 filtration. While using MERV 13 filtration does not reduce the virus concentration as much as supplying 100% outdoor air, it still reduces the annual building-average virus concentration by about 10% compared to using MERV 10 filtration. Use of HEPA filtration only reduces the annual building-average virus concentration by about 5% compared to use of MERV 10 filtration, despite the high-efficiency of

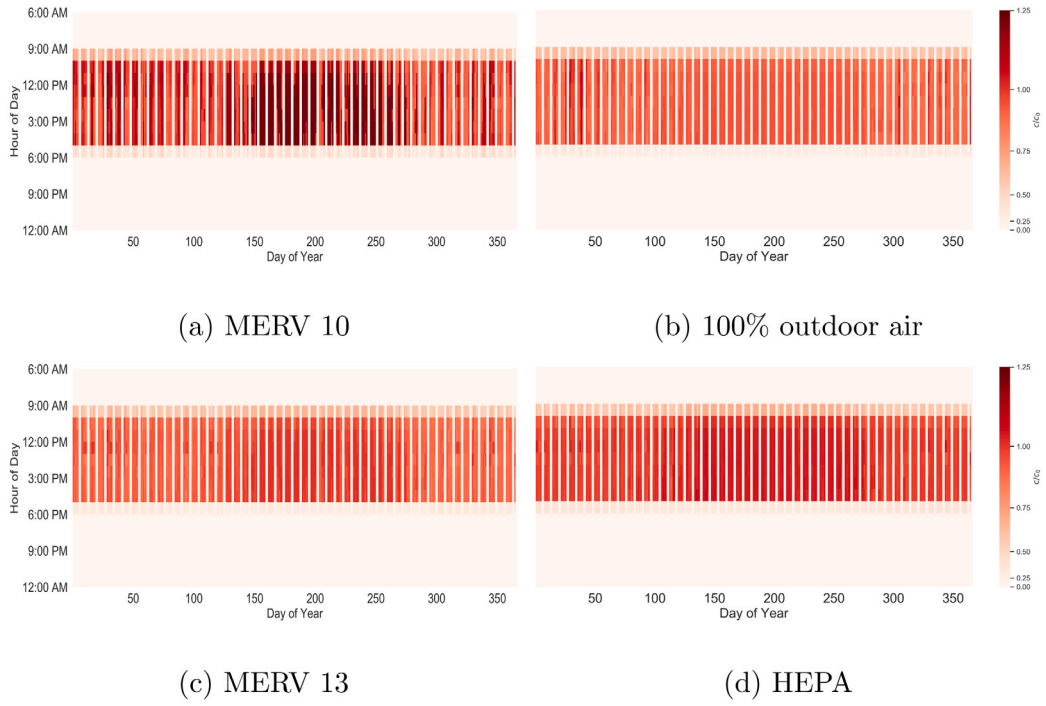

Fig. 8. Heat maps showing the magnitude of normalized concentration during the days over the course of the year.

the HEPA filter. This occurs because the supply fan is not sized for the increased pressure drop when using the HEPA filter, so the airflow supplied to the building is reduced compared to the other strategies. In terms of the concentrations in each of the zones, the Core zone has the lowest average concentration. In large part this is because it is the largest zone but has the same number of sick people as the other zones. The North zone has the highest concentrations for all the strategies due to having the lowest nominal flow rate based on the system sizing. This zone will be used for further analysis in Section 4.1.3.

Fig. 8 shows the variation of concentration for the four strategies during the day throughout the year. For each weekday, the concentration begins to increase at 9:00 AM when the sick people arrive, then decays quickly when they leave at 5:00 PM. The MERV 10 case reveals the increased concentration during the summer and some weeks during the winter when the HVAC system tends to supply the minimum outdoor airflow. In contrast, more outdoor air can be supplied during the mild shoulder seasons to provide free cooling and/or increase ventilation. While the total supply flow rate does not vary significantly throughout the year (for a given strategy), the fraction of supplied outdoor air can vary significantly. The other cases do not show as significant variation during the year, since they are less sensitive to the outdoor air fraction due to their ability to remove virus efficiently.

4.1.2. Monthly virus concentration results

The monthly results for building-average virus concentration for the four strategies are shown in Fig. 9. This further reveals the implications of changing seasons on the virus concentration for the different strategies. While the average concentrations for the use of 100% outdoor air and HEPA filtration vary slightly month-to-month, the MERV 10 case varies more due to its sensitivity to outdoor air fraction. Also, the variation of concentration for the MERV 13 case is more apparent in this figure, since it still does not supply as clean air as the 100% outdoor air and HEPA cases. The results show the lowest average virus concentrations for the MERV 10 and MERV 13 cases occur during April, October, and November when the weather is most mild and the HVAC system tends to supply more outdoor air. Similarly, the highest concentrations for these cases occur during the hot summer months when the system often supplies the minimum outdoor air. This reveals the advantage of supplying 100% outdoor air, relative to using MERV 10 and MERV 13 filtration, during the summer based on the virus concentration. The reduced advantage of the 100% outdoor air case during mild weather, based on the virus concentration, is also apparent.

4.1.3. Sample day virus concentration results

Transient results for virus concentration and risk in the worst zone (North Zone) for two sample days are shown in this section. The emission of virus depends on the individuals and their activities, for example if they are speaking or exercising. To capture that variation, three different virus generation rates (q = 2 quanta/h, 25 quanta/h, and 50 quanta/h) were considered. These generation rates roughly span low, moderate, and higher activity of a sick person.

First, virus concentration results for a hot summer day are shown in Fig. 10. This shows the differences among the strategies when the filter cases use the minimum outdoor supply flow rate. All the strategies follow a similar trend throughout the day. The virus concentration increases at 9:00 AM when the sick people arrive, tends towards an equilibrium during the middle of the day, then sharply decreases when the sick people leave at 5:00 PM. The 100% outdoor air strategy reduces the virus concentration for this day by up to 22% compared to the MERV 10 case. Use of MERV 13 and HEPA filtration reduces the virus concentration by up to 17% and 14%, respectively, compared to MERV 10 filtration for this day. When the virus generation rate is very low, as shown in Fig. 10(a), then the impact of the different strategies is very small due to the low levels of virus concentration.

To better understand the implication of these virus concentrations, the predicted number of infections over time, $R_0(t)$, for this day are shown in Fig. 11. The higher generation rates increase the predicted number of infections, as expected due to the higher virus concentrations. This is because the predicted number of infections accounts for the amount of virus inhaled by the susceptible occupants throughout the day. Both the occupancy and concentration vary throughout the day, so the predicted number of infections is calculated and summed for each hour to account for these dynamic effects. For example, $R_0(t)$ begins to increase at 9:00 AM as the concentration increases and susceptible occupants are exposed to the virus. The slope of $R_0(t)$ then decreases at 12:00 PM when occupants leave for lunch, but the slope

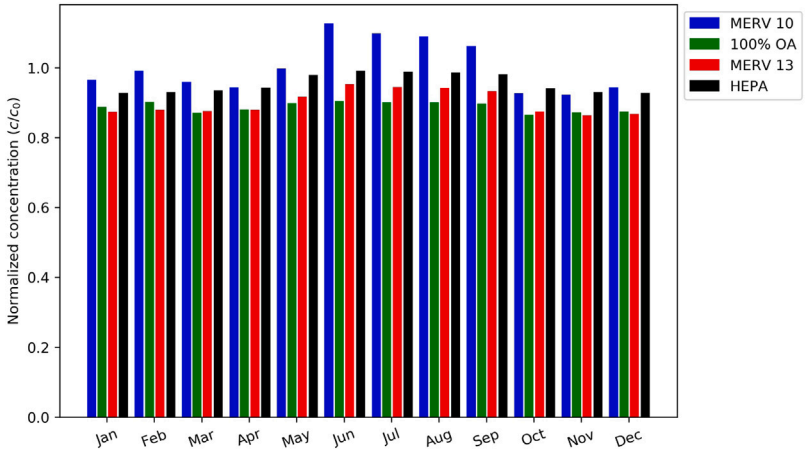

Fig. 9. Monthly building-average virus concentration results for the different strategies.

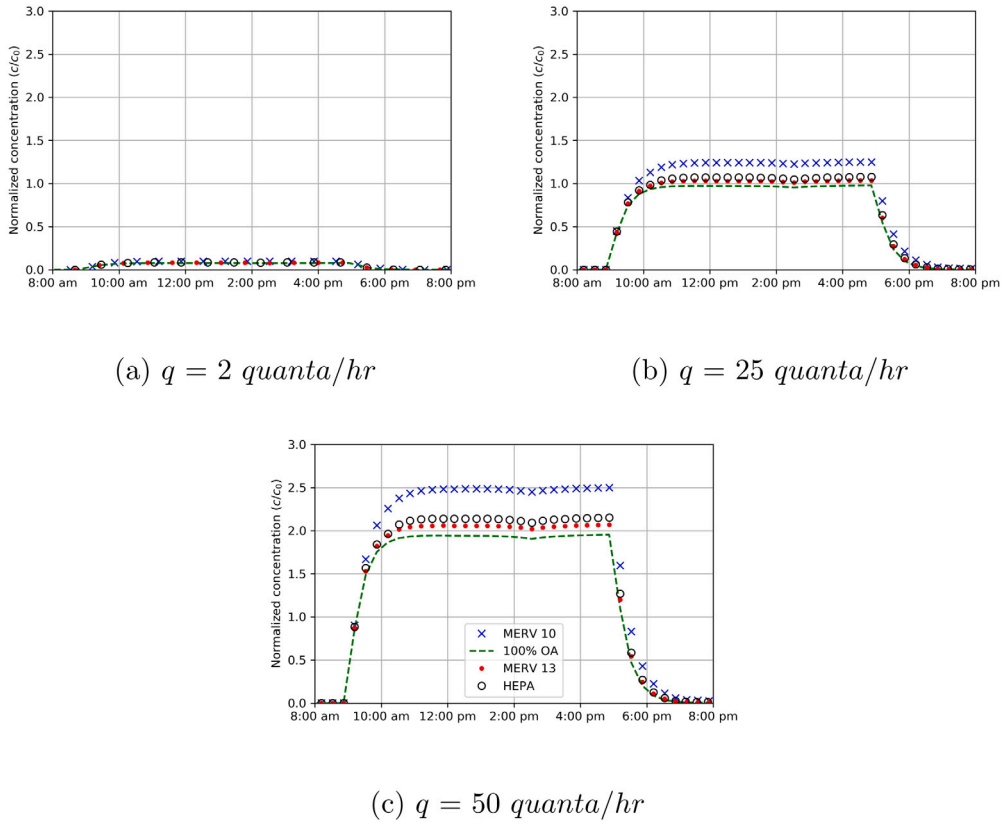

Fig. 10. Normalized virus concentration in the worst zone for a hot day with different virus generation rates.

increases again when they return at 1:00 PM. Finally, $R_0(t)$ flattens out at its final value when the virus concentration decays to zero at the end of the day.

Even for the most effective strategies, it is possible or even very likely that one infection will occur in this zone if the generation rate is high, as shown in Fig. 11(c). For example, R_0 reaches 0.75 at the end of the day for the highest generation rate case with use of 100% outdoor air. This suggests that there is a 75% chance that one person in the zone that day is exposed to a level that could result in an infection. Use of 100% outdoor air offers the benefit of reducing R_0 by about 0.20 at the end of the day when compared to use of MERV 10 filtration. Use of MERV 13 and HEPA filtration reduces R_0 at the end of the day by about 0.15 and 0.13, respectively, compared to MERV 10 filtration. For the medium generation rate, the probability that one infection occurs in the zone for this day is slightly under 50% for the four strategies. R_0 is reduced by about 0.10 at the end of the day for the 100% outdoor air case compared to the MERV 10 case. Use of MERV 13 and HEPA filtration reduces R_0 at the end of the day by about 0.08 and 0.06, respectively, compared to MERV 10 filtration. The relative differences among the strategies are more significant as the generation rate increases, and the relative differences are essentially negligible for the lowest generation rate as shown in Fig. 11(a). For the lowest generation rate, the R_0 at the end of the day for the four strategies is between 0.03 and 0.04, meaning there is a 3%–4% chance one infection occurs in the zone for this day for all the strategies.

Next, the results for virus concentration in the worst zone for a mild spring day are shown. For this day, all the cases supply 100% outdoor air due to the control of the outdoor air economizer during the mild

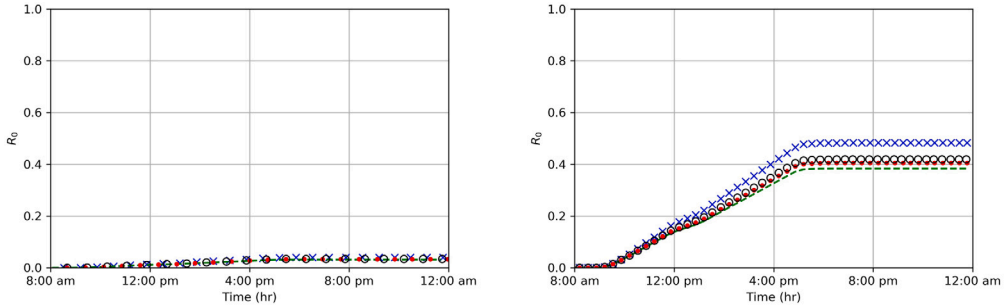

(a) $q = 2\ quanta/hr$ (b) $q = 25\ quanta/hr$

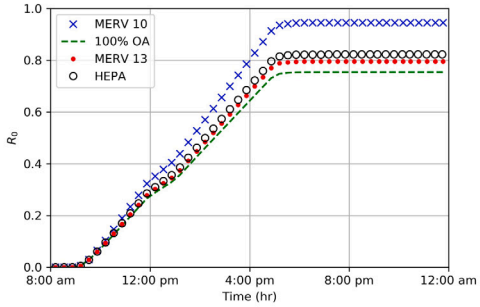

(c) $q = 50\ quanta/hr$

Fig. 11. Predicted number of infections in the worst zone for a hot day with different virus generation rates.

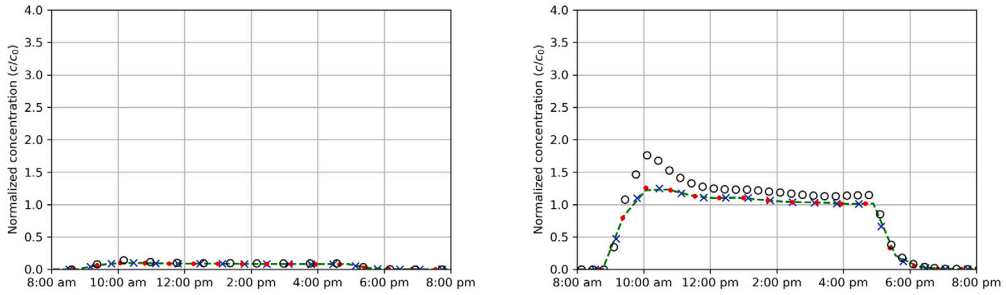

(a) $q = 2\ quanta/hr$ (b) $q = 25\ quanta/hr$

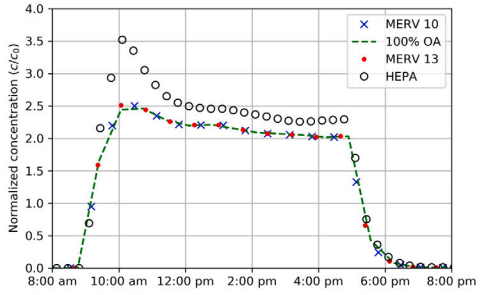

(c) $q = 50\ quanta/hr$

Fig. 12. Normalized virus concentration in the worst zone for a mild day with different virus generation rates.

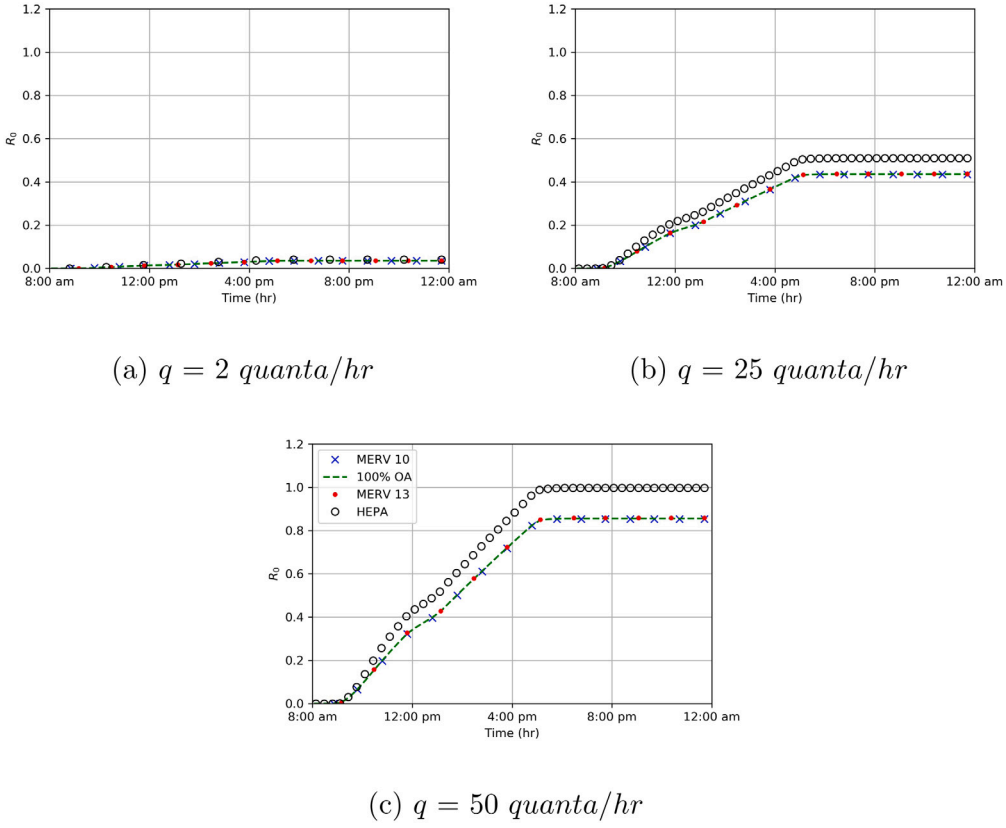

(a) $q = 2\ quanta/hr$

(b) $q = 25\ quanta/hr$

(c) $q = 50\ quanta/hr$

Fig. 13. Predicted number of infections in the worst zone for a mild day with different virus generation rates.

weather. This causes the MERV 10, MERV 13, and 100% outdoor air cases to overlap with each other for these plots. The HEPA filter case does not overlap with the other cases due to the reduced supply flow rate to the zone caused by the increased pressure drop of the HEPA filter. There is also an overshoot in virus concentration around 10:00 AM for the HEPA case. This is due to an initially lower amount of clean airflow to the zone, which eventually increases and settles during the day.

The predicted number of infections for this day are shown next in Fig. 13. Since the concentrations overlap for the cases (excluding HEPA filter) in Fig. 12, it is expected the predicted number of infections also overlap for these cases. Once again, even though these cases supply 100% clean air throughout the day, it is still likely at least one infection occurs during the day in this zone for the highest generation rate. The final value of R_0 for the cases excluding HEPA is about 0.85, meaning there is still about an 85% chance an infection occurs in the zone during this day for the high generation rate. This corresponds to a reduction of R_0 by about 0.15 compared to use of HEPA filtration for this day. For the medium generation rate, the final value of R_0 for the non-HEPA cases is around 0.44 and is about 0.07 lower compared to the HEPA case. Finally, the final value of R_0 is around 0.04 for the four cases with the low generation rate.

4.2. Energy consumption results

The total annual energy consumption for the four different strategies are shown in Table 2, including the breakdown of energy consumption in terms of fan, cooling, and heating energy. The total source energy is also included to show the energy required at the source to provide the site energy. In this study, the fan and cooling devices use electricity while heating is provided with natural gas. The source to site conversion factor is 1.05 for natural gas heating [30] and 2.25 for electricity from the grid based on the breakdown of electricity sources for Denver, CO [31] and their respective conversion factors [32,33]. For this system, the fan energy consumption tends to be most dominant and this energy consumption increases for both the MERV 13 and HEPA filter cases due to the increased pressure drops. The heating energy also tends to be more significant than cooling energy due to Denver's cold climate. This is shown by the large increase in heating energy for the 100% outdoor air case in order to heat the cold outdoor air during the winter, compared to a smaller increase in cooling energy. There is also a decrease in heating energy for the MERV 13 and HEPA filter cases. This is because heat is dissipated to the airflow based on the power drawn from the fan. Thus, more heat is dissipated by the fan as it draws more power for the MERV 13 and HEPA filter cases, which saves some heating energy. This also results in an increase in cooling energy for the MERV 13 and HEPA cases compared to the MERV 10 case.

Due to the increase in heating energy, the 100% outdoor air case consumes about 54% more total site energy than the MERV 10 case and has the highest total site energy consumption among the four strategies. In comparison, use of MERV 13 and HEPA filtration increase the total site energy consumption by about 3% and 12%, respectively, compared to MERV 10 filtration. However, the total source energy for the cases gives a better representation of the cost of energy for the building. Since the MERV 13 and HEPA cases use more electricity to power the fan, they increase the total source energy consumption by about 6% and

Table 2
Annual HVAC energy consumption for the different strategies.

Case	Fan Energy (MWh)	Cooling Energy (MWh)	Heating Energy (MWh)	Total Site Energy (MWh)	Total Source Energy (MWh)
MERV 10 filter	32.8	13.2	26.3	72.3	131.0
100% outdoor air	32.1	14.7	64.3	111.1	172.8
MERV 13 filter	36.7	13.5	24.3	74.5	138.4
HEPA filter	53.4	14.4	12.9	80.7	166.0

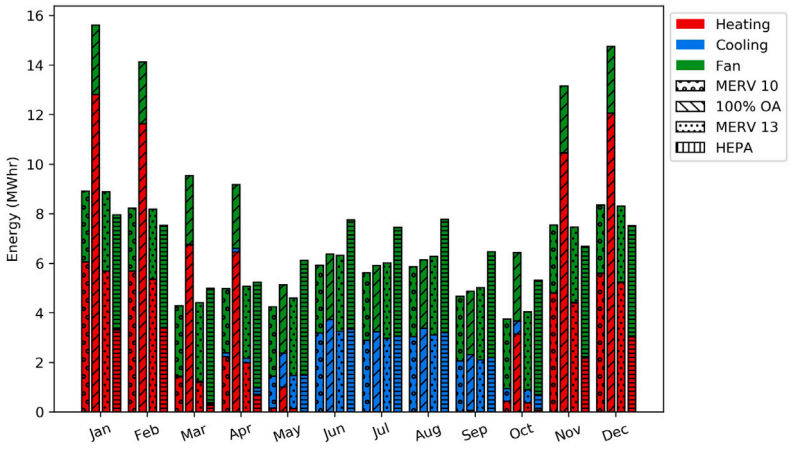

(a) Site energy.

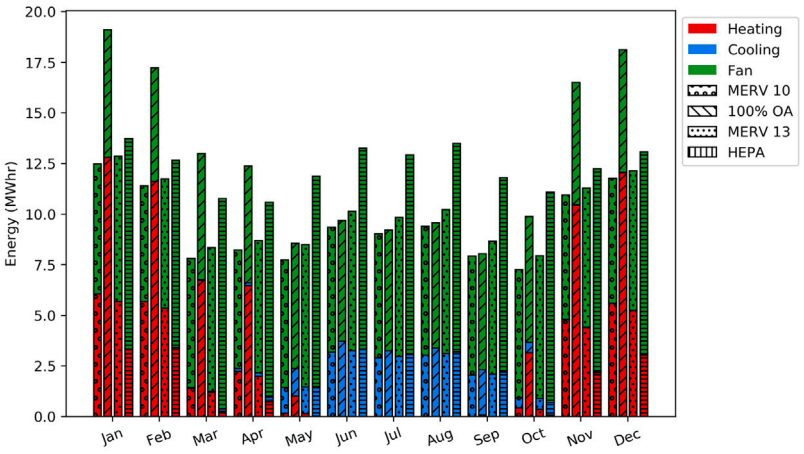

(b) Source energy.

Fig. 14. Monthly breakdown of HVAC energy consumption for the different strategies.

27%, respectively, compared to MERV 10 filtration. In contrast, the energy increase for the 100% outdoor air case is mostly from natural gas heating, so the increase in total source energy consumption is instead about 32%.

The monthly breakdown of energy consumption is shown next in Fig. 14 to compare the operational strategies throughout the year. Both monthly site and source energy are shown. All the cases excluding the HEPA case consume less energy in the warmer months due to the dominance of heating energy for this HVAC system and climate. This is not true for the HEPA case due to the significant amount of heat dissipated by the fan for the high pressure drop filter. The plots show a massive increase in heating energy for the 100% outdoor air case during the colder months, with a less significant increase in cooling energy for the 100% outdoor air case during the summer. The source energy plot shows the more significant increase in energy for the MERV 13 and HEPA filter cases, especially during the summer when mostly electrical energy is used.

4.3. Analysis of combined results

Based on the results for virus concentration, use of 100% outdoor air provides the best overall indoor air quality. Although MERV 13 filtration is slightly less effective, it offers similar levels of improvement in indoor air quality with small increases in risk of infection compared to the 100% outdoor air case. The energy consumption results show similar levels of site energy consumption for the three filter cases, while the 100% outdoor air case consumes more energy at the site compared to the other cases due to the significant increase in heating energy. However, the increase in source energy is more significant for the MERV 13 and HEPA filter cases due to the increase in electricity to power the fan. The increase in source energy consumption is less significant for the 100% outdoor air case since the additional energy is mostly heating provided by natural gas. The final consideration is the cost of the filters. The price of MERV 13 filters can range from $12-$190 depending on the depth and style of filter used [9], while HEPA filters can range from $250–$350.

Based on all these considerations, ASHRAE-recommended MERV 13 filtration performs best due to its improvement in indoor air quality with relatively low operational cost. HEPA filtration could potentially be beneficial if the system is sized to accommodate the increased pressure drop. However, HEPA filtration can have negative effects on both indoor air quality and energy consumption if the system is not sized for it. Additionally, the cost of a HEPA filter is higher than a

MERV 13 filter. Use of 100% outdoor air can be used to provide slightly better indoor air quality compared to MERV 13 filtration. For this climate, it is most beneficial to use in the warmer seasons to avoid the significant increase in heating energy during the winter.

5. Conclusion

Different strategies to improve indoor air quality during the COVID-19 pandemic are investigated for a medium office building in a cold and dry climate. Specifically, the supply of 100% outdoor air and use of filtration with MERV 10, MERV 13, or HEPA ratings are investigated throughout the year using Modelica-based models. The building is modeled using the Modelica *Buildings* library and new models for HVAC filtration and transmission of virus are developed to support this study.

The results show the 100% outdoor air case reduces average virus concentration by about 11% compared to MERV 10 filtration, but consumes significantly more energy at the site compared to the other cases due to the large increase in heating energy during the winter months. Use of MERV 13 filtration reduces the average virus concentration by about 10% compared to MERV 10 filtration and shows similar results for risk compared to the 100% outdoor air case. Use of HEPA filtration did not improve the indoor air quality compared to MERV 13 filtration because of the reduced system flow rate, since the system was not sized for a HEPA filter. The HEPA filter case also used more energy compared to the MERV 13 case because of the increased fan energy. Thus, using ASHRAE-recommended MERV 13 filtration can achieve a good balance between the indoor air quality and operational cost.

In this paper, we develop computational modules and allow for temporal assessment of exposure and risks of indoor occupants. We demonstrate how such an approach allows one to consider the various tradeoffs between exposure risk, HVAC capacity, and energy use. We also show how to consider the marginal benefits of such tradeoffs for current crises and will thus be available if future what-if scenarios are to be considered.

Declaration of competing interest

The authors declare that they have no known competing financial interests or personal relationships that could have appeared to influence the work reported in this paper.

Acknowledgments

This research was supported in part by the U.S. Defense Threat Reduction Agency and performed under U.S. Department of Energy Contract No. DE-AC02-05CH11231. This work emerged from the IBPSA Project 1, an international project conducted under the umbrella of the International Building Performance Simulation Association (IBPSA). Project 1 will develop and demonstrate a BIM/GIS and Modelica Framework for building and community energy system design and operation.

References

[1] H. Qian, T. Miao, L. Liu, X. Zheng, D. Luo, Y. Li, Indoor transmission of SARS-CoV-2, Indoor Air 31 (3) (2021) 639–645.
[2] F.R. Lendacki, R.A. Teran, S. Gretsch, M.J. Fricchione, J.L. Kerins, COVID-19 Outbreak among attendees of an exercise facility — Chicago, illinois, August–September 2020, Morb. Mortal. Wkly. Rep. 70 (9) (2021) 321–325.
[3] J. Lu, J. Gu, K. Li, C. Xu, W. Su, Z. Lai, D. Zhou, C. Yu, B. Xu, Z. Yang, COVID-19 Outbreak associated with air conditioning in restaurant, Guangzhou, China, 2020, Emerg. Infect. Diseases 26 (7) (2020) 1628–1631.
[4] ASHRAE Epidemic Task Force, Core recommendations for reducing airborne infectious aerosol exposure, ASHRAE (2021).
[5] J. Zhang, D. Huntley, A. Fox, B. Gerhardt, A. Vatine, J. Cherne, Study of viral filtration performance of residential HVAC filters, ASHRAE J. 62 (8) (2020) 26–32.
[6] M. Zaatari, A. Novoselac, J. Siegel, The relationship between filter pressure drop, indoor air quality, and energy consumption in rooftop HVAC units, Build. Environ. 73 (2014) 151–161.
[7] H.R.R. Santos, V.M.S. Leal, Energy vs. ventilation rate in buildings: A comprehensive scenario-based assessment in the European context, Energy Build. 54 (2012) 111–121.
[8] M. Zaatari, A. Novoselac, J. Siegel, Impact of ventilation and filtration strategies on energy consumption and exposures in retail stores, Build. Environ. 100 (2016) 186–196.
[9] T. Ben-David, M.S. Waring, Interplay of ventilation and filtration: Differential analysis of cost function combining energy use and indoor exposure to PM2.5 and ozone, Build. Environ. 128 (2018) 320–335.
[10] P. Azimi, B. Stephens, HVAC Filtration for controlling infectious airborne disease transmission in indoor environments: Predicting risk reductions and operational costs, Build. Environ. 70 (2013) 150–160.
[11] H. Bohanon, M. Zaatari, Effect of ventilation and filtration on viral infection in residences, ASHRAE J. 62 (12) (2020) 38–45.
[12] L.F. Pease, N. Wang, T.I. Salsbury, R.M. Underhill, J.E. Flaherty, A. Vlachokostas, G. Kulkarni, D.P. James, Investigation of potential aerosol transmission and infectivity of SARS-CoV-2 through central ventilation systems, Build. Environ. 197 (2021) 107633.
[13] Y. Fu, W. Zuo, M. Wetter, J.W. VanGilder, P. Yang, Equation-based object-oriented modeling and simulation of data center cooling systems, Energy Build. 198 (2019) 503–519.
[14] S. Huang, W. Zuo, D. Vrabie, R. Xu, Modelica-based system modeling for studying control-related faults in chiller plants and boiler plants serving large office buildings, J. Build. Eng. 44 (2021) 102654.
[15] W. Tian, X. Han, W. Zuo, Q. Wang, Y. Fu, M. Jin, An optimization platform based on coupled indoor environment and HVAC simulation and its application in optimal thermostat placement, Energy Build. 199 (2019) 342–351.
[16] M. Wetter, W. Zuo, T.S. Nouidui, X. Pang, Modelica buildings library, J. Build. Perform. Simul. 7 (4) (2014) 253–270.
[17] M. Wetter, M. Bonvini, T.S. Nouidui, W. Tian, W. Zuo, Modelica Buildings Library 2.0, in: Proceedings of BS2015: 14th Conference of International Building Performance Simulation Association, 2015.
[18] M. Guo, P. Xu, T. Xiao, R. He, M. Dai, S.L. Miller, Review and comparison of HVAC operation guidelines in different countries during the COVID-19 pandemic, Build. Environ. 187 (2021) 107368.
[19] ASHRAE, Standard 52.2. Method of testing general ventilation air-cleaning devices for removal efficiency by particle size, Am. Soc. Heat. Refrig. Air Cond. Eng. (2017).
[20] R.W. Fox, Air cleaners: a review, J. Allergy Clin. Immunol. 94 (2) (1994) 413–416.
[21] Buildings.Examples.VAVReheat, 2013, https://simulationresearch.lbl.gov/modelica/releases/v5.0.0/help/Buildings_Examples_VAVReheat.html#Buildings.Examples.VAVReheat.
[22] Department of Energy, Commercial Reference Buildings, https://www.energy.gov/eere/buildings/commercial-reference-buildings.
[23] ASHRAE, Standard 62.1 ventilation for acceptable indoor air quality, Am. Soc. Heat. Refrig. Air Cond. Eng. (2015).
[24] M. Wetter, J. Hu, M. Grahovac, B. Eubanks, P. Haves, Openbuildingcontrol: Modeling feedback control as a step towards formal design, specification, deployment and verification of building control sequences, in: Proceedings of 2018 Building Performance Modeling Conference and SimBuild, 2018.
[25] T. Xia, C. Chen, Evolution of pressure drop across electrospun nanofiber filters clogged by solid particles and its influence on indoor particulate air pollution control, J. Hard Mater. 402 (2021) 123479.
[26] Dwyer, MERV 10 Pleated Filters, https://www.dwyer-inst.com/PDF_files/Priced/DF10_cat.pdf.
[27] Dwyer, MERV 13 Pleated Filters, https://www.dwyer-inst.com/PDF_files/Priced/DF13_cat.pdf.
[28] G. Buonanno, L. Stabile, L. Morawska, Estimation of airborne viral emission: Quanta emission rate of SARS-CoV-2 for infection risk assessment, Environ. Int. 141 (2020) 105794.
[29] G. Buonanno, L. Morawska, L. Stabile, Quantitative assessment of the risk of airborne transmission of SARS-CoV-2 infection: prospective and retrospective applications, Environ. Int. 145 (2020) 106112.
[30] EnergyStar, Source energy, Energy Star Portfolio Manag. (2020) 1–19.
[31] U.S. Energy Information Administration, Colorado net electricity generation by source, 2021, https://www.eia.gov/state/?sid=CO#tabs-4.
[32] L.N. Troup, D.J. Fannon, M.J. Eckelman, Spatio-temporal changes among site-to-source conversion factors for building energy modeling, Energy Build. 213 (2020) 109832.
[33] X. Zhang, N.P. Myhrvold, K. Caldeira, Key factors for assessing climate benefits of natural gas versus coal electricity generation, Environ. Res. Lett. 9 (11) (2014) 114022.